Lab on a Chip

Accepted Manuscript

ROYAL SOCIETY OF CHEMISTRY

www.rsc.org/loc

SIMULTANEOUS CONCENTRATION AND DETECTION OF BIOMARKERS ON PAPER*

Ricky Y. T. Chiu, Erik Jue, Allison T. Yip, Andrew R. Berg, Stephanie J. Wang, Alexandra R. Kivnick, Phuong T. Nguyen, and Daniel T. Kamei

Department of Bioengineering, University of California, Los Angeles, CA

420 Westwood Plaza

5121J Engineering V, P.O. Box 951600

University of California

Los Angeles, CA 90095-1600

Abstract

The lateral-flow immunoassay (LFA) is an inexpensive point-of-care (POC) paper-based diagnostic device with the potential to rapidly detect disease biomarkers in resource-poor settings. Although LFA is inexpensive, easy to use, and requires no laboratory equipment, it is limited by its sensitivity, which remains inferior to that of gold standard laboratory-based assays. Our group is the only one to have previously utilized various aqueous two-phase systems (ATPSs) to enhance LFA detection. In those studies, the sample was concentrated by an ATPS in a test tube and could only be applied to LFA after it had been extracted manually. Here, we bypass the extraction step by seamlessly integrating a polyethylene glycol-potassium phosphate ATPS with downstream LFA detection in a simple, inexpensive, power-free, and portable all-in-one diagnostic device. We discovered a new phenomenon in which the target biomarkers simultaneously concentrate as the ATPS solution flows through the paper membranes, and our device features a 3-D paper well that was designed to exploit this phenomenon. Studies with this device, which were performed at room temperature in under 25 min, demonstrated a 10-fold improvement in the detection limit of a model protein, transferrin. Our next-generation LFA technology is rapid, affordable, easy-to-use, and can be applied to existing LFA products, thereby providing a new platform for revolutionizing the current state of disease diagnosis in resource-poor settings.

Keywords

3-D paper-based diagnostic device, dextran-coated gold nanoprobes, aqueous two-phase systems, lateral-flow immunoassay

Introduction

Over 95% of deaths due to major infectious diseases (HIV, malaria, acute respiratory infections, and tuberculosis) occur in resource-poor countries.[1] There is a critical need for earlier detection of these diseases as it can lead to better patient management, faster administration of treatments, and improved outbreak prevention.[2] However, the current diagnostic technologies capable of providing rapid and accurate detection are not readily available in developing nations due to limited access to electricity, laboratory equipment, and trained personnel.[3] To overcome these challenges, resource-poor countries need an equipment-free diagnostic assay that is rapid, simple to use, low-cost, easy to interpret, and applicable at the point-of-care (POC).[4] A paper-based analytical device has the potential to satisfy the aforementioned criteria since paper is readily available, affordable, and possesses an intrinsic wicking mechanism that can quickly transport fluids without the aid of an active pumping system. One common paper-based diagnostic device is the lateral-flow immunoassay (LFA), a rapid antibody-based test that has been used successfully in off-the-counter pregnancy tests and urine drug test kits. Despite its strengths as a POC device, the detection limit of LFA is still inferior in comparison to that of gold-standard diagnostic laboratory assays such as the enzyme-linked immunosorbent assay (ELISA) and polymerase chain reaction (PCR).[1]

The Whitesides and Yager groups have developed novel methodologies to improve detection in paper-based devices. Specifically,[5, 6] the Whitesides group developed a low-cost paper-based ELISA with multiple wash and reagent steps that brings its detection limit close to that of traditional ELISA.[7] Meanwhile, the Yager group developed a two-dimensional paper network

format featuring easily performed multi-step signal amplification assays that yield a 4-fold improvement in the detection limit. There have also been a number of studies investigating flow rates[8, 9] and timed delays[10-13] which may lead to the improved automation and ease-of-use of paper-based fluidic devices. Concurrently, our group was the first to demonstrate that an aqueous two-phase system (ATPS) can be used to concentrate a target biomarker into a smaller volume before addition to LFA. Using this method, a 10-fold improvement in the overall detection limit of LFA was achieved for a model virus bacteriophage M13 and a model protein transferrin (Tf).[14, 15] However, this approach was also limited by its time-to-result and ease-of-use, as the user had to wait for the two phases of the ATPS to macroscopically separate before extracting the target phase containing the concentrated biomarker and applying it to LFA.

Here we improve sensitivity, speed, and ease-of-use with a next-generation, all-in-one device possessing both ATPS phase separation and downstream detection capabilities. Instead of applying the concentrated sample after phase separation of the ATPS, device revolves around a new phenomenon we discovered, which enables the direct addition of a mixed ATPS to the paper-based device. The solution separates into its two phases as it flows towards the detection zone, allowing for the concentration and detection steps to occur simultaneously and further reducing the overall time-to-result. Although the precise mechanism is still under investigation, our studies on this newly discovered concentrating phenomenon suggest that the paper membrane speeds up the macroscopic phase separation of the ATPS. To further capitalize on this phenomenon, we expanded the paper device vertically, thereby increasing the cross-sectional area of flow and exploiting the effects of gravity on macroscopic separation. In addition to accelerating phase separation, this 3-D component also has the ability to process larger, more dilute volumes of sample, leading to greater concentration-fold improvements. This is the first

time that phase separation in paper has been investigated, and the novel integration of ATPS and LFA within a 3-D paper architecture successfully yielded a 10-fold improvement in the detection limit of our model protein Tf, while reducing the overall time-to-result and maintaining ease-of-use. Our device provides a significant improvement over traditional LFA tests and can be modified for the detection of a variety of diseases with low characteristic biomarker levels. This new platform technology is highly sensitive, low-cost, rapid, equipment-free, and therefore has the potential to revolutionize the current state of diagnostic healthcare within resource-poor regions.

Materials and Methods

Determining the Polymer-Salt ATPS Solution Volume Ratios

All materials, chemicals, and reagents were purchased from Sigma-Aldrich (St. Louis, MO) unless otherwise noted. Polyethylene glycol 8000 (PEG, VWR, Brisbane, CA) and potassium phosphate salt (5:1 dibasic to monobasic ratio) were dissolved in Dulbecco's phosphate-buffered saline (PBS; Invitrogen, Grand Island, NY, pH 7.4, containing 1.47 mM KH_2PO_4, 8.1 mM Na_2HPO_4, 137.92 mM NaCl, 2.67 mM KCl, and 0.49 mM $MgCl_2$). The equilibrium volume ratios (volume of the top phase divided by the volume of the bottom phase) were obtained by varying the w/w compositions of PEG and salt along the same tie line. The 1:1 and 9:1 volume ratio ATPSs were found and used for further experiments.

Preparation of Antibody-Decorated Dextran-Coated Gold Nanoprobes (DGNPs)

Dextran-coated gold nanoparticles were synthesized according to Min and coworkers with slight modifications.[16] Briefly, 6 g of dextran (Mw. 15,000 – 25,000) from *Leuconostoc* spp. were

dissolved in 80 mL of filtered UltraPure sterile water (Rockland Immunochemicals Inc., Gilbertsville, PA). The solution was stirred and heated to a boil, after which 1080 µL of a 1% w/v gold (III) chloride hydrate solution were added. The color of the reaction mixture turned reddish-violet and was stirred and boiled for about 20 min. The newly formed dextran-coated gold nanoparticles were centrifuged to remove free dextran and resuspended in 70 mL of water. To form functionalized DGNPs, the pH of the dextran-coated gold nanoparticle solution was adjusted to 9.0 using 1.5 M NaOH. For every 1 mL of dextran-coated gold nanoparticle solution, 8 µg of anti-Tf antibodies (Bethyl Laboratories, Montgomery, TX) were added. The reaction mixture was placed on a shaker for 30 min to facilitate the formation of dative bonds between the antibodies and the dextran-coated gold nanoparticles. Free antibodies were removed by centrifugation. The pellet was resuspended in 100 µL of 0.1 M sodium borate buffer at pH 9.0.

Visualization of ATPS

In order to visualize the two phases of the ATPS, dextran-coated gold nanoparticles, which are purple due to surface plasmon resonance,[17, 18] and Brilliant Blue FCF dye (The Kroger Co., Cincinnati, OH) were added to 3 g total PBS solutions containing the previously determined concentrations of PEG and salt for the 1:1 and 9:1 volume ratios. These solutions were well-mixed through vortexing and incubated at 25 °C. Pictures of the solutions were taken when the ATPS reached equilibrium. All images were captured using a Canon EOS 1000D camera (Canon U.S.A., Inc., Lake Success, NY).

The two phases of the ATPS were then visualized as they flowed along a paper membrane. Two 8 x 30 mm strips of fiberglass paper were laser cut with a VersaLASER 3.50 (Universal Laser

Systems, Scottsdale, AZ). Subsequently, 50 mg of the mixed ATPS (corresponding to the 1:1 or 9:1 equilibrium volume ratio) containing Brilliant Blue FCF dye and dextran-coated gold nanoparticles were added drop-wise to one end of the strips using a pipette. Images of the resulting flow were captured at 0, 30, 105, and 300 sec. Video was also taken with a 8-megapixel camera from a commercial smart phone (Apple Inc., Cupertino, CA).

To visualize the phase separation of the ATPS within the 3-D paper well, 140 mg of a mixed ATPS containing Brilliant Blue FCF dye and dextran-coated gold nanoparticles were added to the paper well. The 3-D paper well was formed by stacking nine 8 x 10 mm laser-cut strips of fiberglass paper on one edge of an 8 x 60 mm laser-cut strip of fiberglass. After the mixed ATPS was applied to the 3-D paper well, 50 μL of running buffer (0.2% bovine serum albumin (BSA), 0.3% Tween20, 0.1 M Trizma base, pH 8) were added to the 3-D paper well. A running buffer was added to assist the flow of the sample from the paper well to the rest of the device. Video was taken and images were captured at 0 and 30 sec, at the addition of running buffer, and after completion of flow.

Detection of Tf

LFA Tests for Detection of Tf

LFA test strips utilizing the competition assay format were assembled similar to our previous studies.[15] Briefly, DGNPs decorated with anti-Tf antibodies were first added to the sample solution, and allowed to bind any Tf present in the sample to form DGNP/Tf complexes. To verify the detection limit of Tf with LFA, 30 μL of running buffer and 20 μL of sample solution, which consists of 15 μL of a known amount of Tf in PBS and 5 μL of the DGNPs, were mixed in a test tube. The LFA test strip was inserted vertically into the tube with the sample pad

submerged in the sample, and the fluid wicked through the strip towards the absorbance pad. If Tf is present, the DGNP/Tf complexes moving through the LFA strip cannot bind to the Tf immobilized on the test line, indicating a positive result with the presence of a single band at the control line. Alternatively, if Tf is not present, antibodies on DGNPs can bind to Tf on the test line. Since these probes exhibit a purplish red color, a visual band forms as the DGNPs accumulate at the test line, indicating a negative result. Regardless of the presence of Tf, the antibodies on DGNP will always bind to the secondary antibodies immobilized on the control line. A band at the control line signifies that the sample flowed completely through the strip, indicating a valid test. Therefore, a negative result is indicated by two bands: one at the test line and one at the control line. In contrast, a positive result is indicated by a single band at the control line. Each Tf concentration was tested in triplicate. The representative LFA strips were imaged by a Canon EOS 1000D camera in a controlled lighting environment after 10 min.

Detection of Tf with the 3-D Paper Well

The LFA component of the paper-based device was slightly modified from the aforementioned setup. Specifically, the cellulose sample pad was replaced with a 5 x 20 mm fiberglass paper, which connected a nitrocellulose membrane containing the test and control lines. At the beginning of the sample pad, a 3-D paper well composed of multiple strips of fiberglass paper was used. For experiments using the 1:1 volume ratio ATPS, the well was composed of five (four 5 x 7 mm strips plus the bottom sample pad) layers of fiberglass paper. To start the test, 40 μL of the mixed 1:1 volume ratio ATPS containing a known concentration of Tf were added to the paper well, followed by the addition of 50 μL of running buffer. Images were captured after 10 min. For experiments using the 9:1 volume ratio ATPS, 20 layers of paper (nineteen 5 x 7 mm strips plus the bottom sample pad) were used to form the paper well. 200 μL of the mixed 9:1

volume ratio ATPS containing a known concentration of Tf were added to the paper well, and allowed to incubate for 10 min, followed by the addition of 100 μL of running buffer. After another 10 min, images were captured by a Canon EOS 1000D camera in a controlled lighting environment. Each Tf concentration was tested in triplicate.

Results and Discussion

Visualization of ATPS

We hypothesized that the integration of ATPS with LFA could significantly improve the detection limit of a traditional LFA test without sacrificing its advantages. To achieve this, it was first necessary to identify an ATPS whose phases could be visualized as it flowed through the paper membrane. Specifically, we used a PEG-salt ATPS, which forms a more hydrophobic, PEG-rich phase on top and a more dense and hydrophilic, PEG-poor phase on bottom. Biomolecule partitioning in the ATPS is primarily dictated by relative hydrophilicity (since biomolecules tend to prefer the phase in which they experience the greatest attractive interactions) and size (since large biomolecules typically do not remain in the PEG-rich phase due to experiencing greater steric excluded-volume repulsive interactions with the greater number of PEG molecules in the PEG-rich phase). Brilliant Blue FCF dye was added to the mixed ATPS, and because it is small and hydrophobic, the dye partitioned extremely into the PEG-rich phase. Purple dextran-coated gold nanoparticles were also added to the mixed ATPS, and partitioned extremely into the PEG-poor phase because they are large (~50 nm diameter as measured by dynamic light scattering) and hydrophilic. Images of a 1:1 volume ratio ATPS and of a 9:1 volume ratio ATPS were taken before and after phase separation (Fig. 1). The amounts of Brilliant Blue FCF and dextran-coated gold nanoparticles were held constant between the 1:1

and the 9:1 volume ratio ATPSs. As a result, after phase separation, the top phase of the 9:1 volume ratio ATPS was greater in volume and therefore less concentrated with blue dye compared to the top phase of the 1:1 volume ratio ATPS. Additionally, the bottom phase of the 9:1 volume ratio ATPS was much smaller in volume and displayed a darker shade of purple than that of the 1:1 volume ratio ATPS, demonstrating that shrinking the bottom phase can effectively concentrate the dextran-coated gold nanoparticles within the ATPS. As shown previously, we expected the 9:1 volume ratio ATPS sample to concentrate the nanoparticles by 10-fold since the volume of the bottom phase becomes 1/10 the volume of the total sample solution. Note that, as the volume ratios become more extreme, greater concentration-fold improvements are attainable but the system also requires more time to separate.

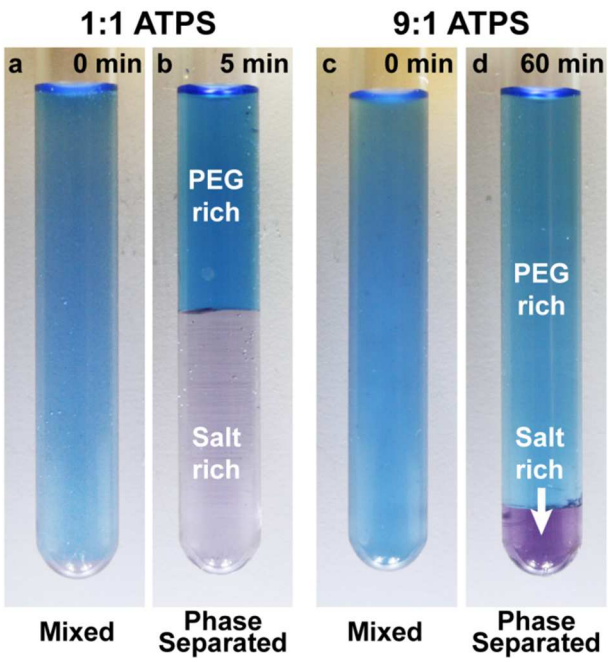

Figure 1: *Brilliant Blue FCF dye and dextran-coated gold nanoparticles partition extremely to the upper PEG-rich and lower PEG-poor phases, respectively.* (a) At 25 °C, a mixed 1:1 volume ratio ATPS phase separated to form (b) two equal volume phases. (c) At 25 °C, a mixed 9:1 volume ratio ATPS phase

separated into (d) a larger PEG-rich phase and a smaller PEG-poor phase. The same amounts of Brilliant Blue FCF and dextran-coated gold nanoparticles were added to both ATPSs. The darker purple color of the 9:1 volume ratio ATPS indicates that the gold nanoparticle concentration in the bottom PEG-poor phase has significantly increased.

Visualization of ATPS in Paper

After adding a mixed ATPS onto the paper membrane, the PEG-poor phase containing the purple dextran-coated gold nanoparticles was observed to flow quickly through the paper. Meanwhile, the PEG-rich phase containing the blue dye was retained at the beginning of the paper membrane (Fig. 2 and Paper Membrane Supplementary Videos, ESI). This result was similar to the case in which both phases of the ATPS were allowed to fully separate inside a glass well before flow through the paper was triggered (Fig. S1 and Triggered Well Supplementary Videos, ESI). The enhanced phase separation occurring within the paper membrane was apparent when using the 1:1 volume ratio ATPS (Fig. 2a), and the 1:1 volume ratio ATPS phase separated almost immediately within the paper. From our previous studies,[19] and as shown in Fig. 1, the fold-concentration of the purple dextran-coated gold nanoparticles achieved using the ATPS is a function of the volume ratio. Specifically, since the particles partition extremely to the PEG-poor phase, a 1:1 volume ratio should yield a 2-fold concentration of the particles as they are flowing in half of the initial volume as the leading front of the flow. One possible explanation of the phase separation behavior in paper membranes is that the PEG-rich domains experience more interactions with the paper, making them less mobile. Furthermore, the PEG-rich domains are also more viscous and thus may experience greater difficulty traveling through the tortuous paper network. In contrast, the PEG-poor domains interact less with the paper and are less viscous,

allowing them to travel quickly through the paper network and coalesce at the leading front. For the 9:1 volume ratio ATPS, the PEG-poor domains comprised only one-tenth of the total volume, making it more difficult for them to coalesce and flow ahead of the PEG-rich domains. Specifically, the time required for macroscopic phase separation to occur in paper was longer than the time it took for the fluid to wick the paper, and a good separation was not observed (Fig. 2b).

When using both the 1:1 and 9:1 volume ratio ATPSs, it was also observed that some PEG-poor domains did not make it to the leading front of flow. This indicated that not all of the PEG-poor domains were able to escape from the PEG-rich domains and explained why the equilibrium volume ratio measured in the test tube did not match the wicking distance ratio on the paper membrane. In order to improve LFA, most of the PEG-poor domains needed to reach the macroscopic PEG-poor phase and separate from the macroscopic PEG-rich phase before reaching the detection zone. Therefore, an additional component was required to further improve the phase separation phenomenon.

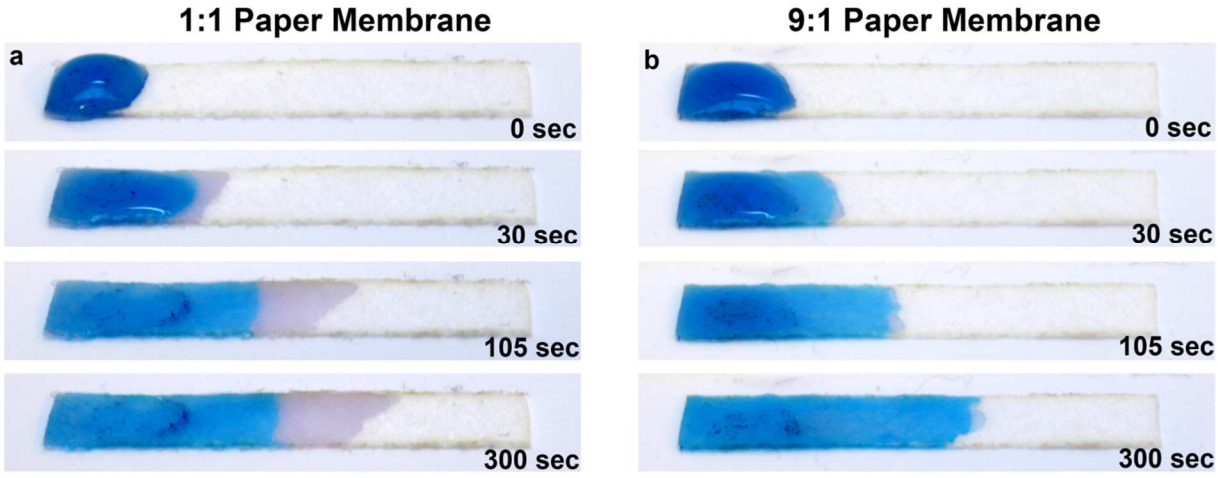

Figure 2: *The paper membrane allows for ATPS phase separation to occur as it flows.* The PEG-rich

domains were retained near the beginning of the paper membrane while the PEG-poor domains moved quickly to the leading front. (a) The 1:1 volume ratio ATPS phase separated and flowed through the paper membrane within 5 min. (b) The 9:1 volume ratio ATPS also separated and flowed through the membrane within 5 min, but the phase separation was less efficient as the leading front is less distinct at 300 sec.

Visualization of ATPS in the 3-D Paper Well Device

A paper well that takes advantage of 3-D paper architectures was designed to further enhance the phase separation behavior. Using a 3-D paper well allows gravitational forces, which normally drive phase separation in test tubes, to also aid in ATPS phase separation within the paper. The 3-D paper architecture also increases the cross-sectional area normal to the direction of flow. More volume can therefore wick through the paper at the same time, allowing more PEG-rich domains to be held back by their interactions with the paper and the PEG-poor domains to coalesce more easily. We show in Fig. 3 and in the 3-D Paper Well Supplementary Videos (ESI) that the 3-D paper well contributed to greater phase separation efficiency over the 2-D paper membrane shown previously. The PEG-rich domains were retained in the top layers of the paper well while the PEG-poor domains containing the concentrated dextran-coated gold nanoparticles flowed towards the bottom layers of the paper well. Additionally, the PEG-poor domains were the first to leave the paper well and were effectively separated from the PEG-rich domains. A running buffer was also added to further drive fluid flow and to help flush any remaining PEG-poor domains through the paper well, and we envision that this addition can be automated in the future. Note that flow was slower when using the 9:1 volume ratio ATPS (the solution does not reach the end of the strip after 390 sec) since there was a greater volume of the more viscous PEG-rich phase.

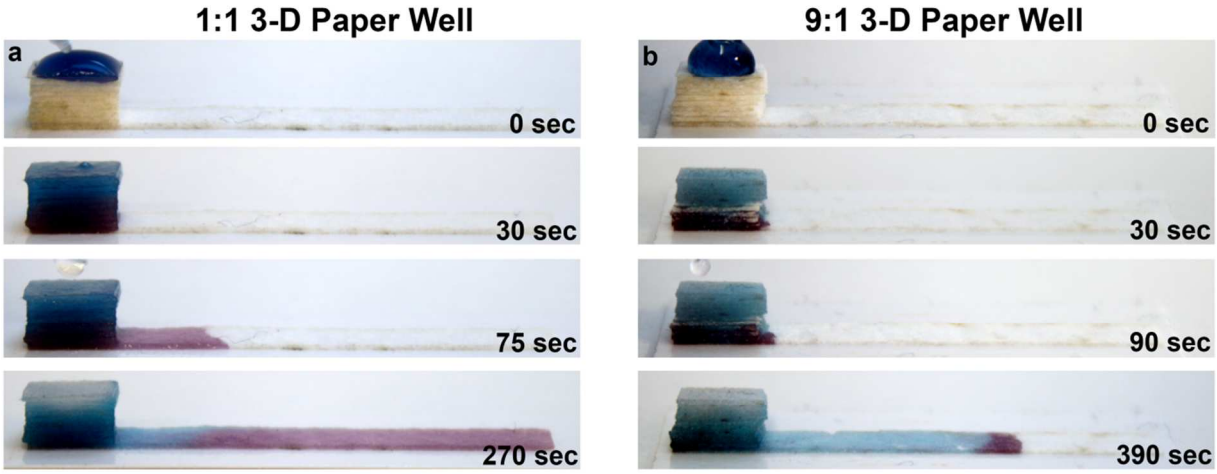

Figure 3: *The 3-D paper well allows for further enhanced ATPS phase separation.* Following the addition of a mixed ATPS with dyes, the PEG-rich domains were retained in the upper layers of the well while the PEG-poor domains containing the concentrated gold nanoparticles flowed quickly to the bottom layers. (a) The 1:1 volume ratio ATPS showed enhanced phase separation in the 3-D paper well and the PEG-poor phase flowed through the membrane within 5 min. (b) The 9:1 volume ratio ATPS also has improved phase separation and the PEG-poor phase was clearly visible. In contrast to Fig. 2, the leading front is well defined and has a dark purple color, signifying concentration of the dextran-coated gold nanoparticles.

Detection of Tf Using the 3-D Paper Well Device

After visualizing the improved ATPS phase separation and flow behavior within the 3-D paper well device, we wanted to determine if LFA could be combined with this technology to improve the detection limit. The Brilliant Blue FCF dye was no longer used, and functionalized anti-Tf DGNPs were used in place of the dextran-coated gold nanoparticles. The DGNPs partition similarly to the dextran-coated gold nanoparticles in the ATPS, but can also capture target biomarkers in the sample and act as the colorimetric indicator for LFA.

We first identified the detection limit for the LFA only control that did not incorporate the ATPS

and 3-D paper well device. To improve the detection limit of LFA relative to the control in the competition format, the antibodies decorated on the DGNPs need to be bound to more Tf. This can be achieved by exposing the same number of DGNPs to a greater number of Tf molecules, and for a fixed concentration of Tf, the total volume of the solution would need to be increased. Although the DGNPs can be saturated with the increase in total volume, they are diluted by the fold-increase in volume. Since each of our LFA strips could handle only 20 μL of sample, due to diluting the DGNPs, an invalid test would result as not enough DGNPs would be bound to the control line. However, when using the ATPS and 3-D paper well device, the DGNPs saturated with Tf molecules partitioned extremely into the PEG-poor phase and could therefore be concentrated in the leading front of the flow on the paper, so that a valid test would result. Accordingly, the sample volume was increased 2-fold to 40 μL when using the 1:1 volume ratio ATPS that was expected to concentrate the DGNPs by 2-fold, leading to the same number of DGNPs entering the detection zone when compared to the control. Similarly, the sample volume was increased 10-fold to 200 μL when using the 9:1 volume ratio ATPS that was expected to concentrate the DGNPs by 10-fold. Since only the bottom phases of the 1:1 and 9:1 volume ratio ATPSs containing the DGNPs should pass through the detection zone, the device's volume processing capacity was fine-tuned by varying the number of layers comprising the 3-D paper well. To accommodate this increase in sample volume, the 3-D paper well used for the detection of Tf within a 1:1 volume ratio ATPS solution was composed of 5 layers of paper, while that for the 9:1 volume ratio ATPS solution was increased to 20 layers of paper (Fig. 4) to accommodate the increased volume. Despite the significant increase in the number of layers, the 3-D paper well for the 9:1 volume ratio ATPS still remained relatively small in comparison to a dime.

When the ATPS solution containing DGNPs was added to the paper well, the DGNPs concentrated rapidly to the leading front of the solution as they wicked through our device. The DGNPs reached the detection region of the device before the remainder of the solution that was retained in the paper well. For the competition assay, the presence of the test line indicates a negative result, whereas the absence of the test line indicates a positive result. When using the negative control which does not contain the model protein Tf, in less than 25 min, both setups using the 1:1 and 9:1 volume ratio ATPSs rendered a visible band at both the test and control lines, respectively, indicating the absence of Tf and a valid test (Fig. 4).

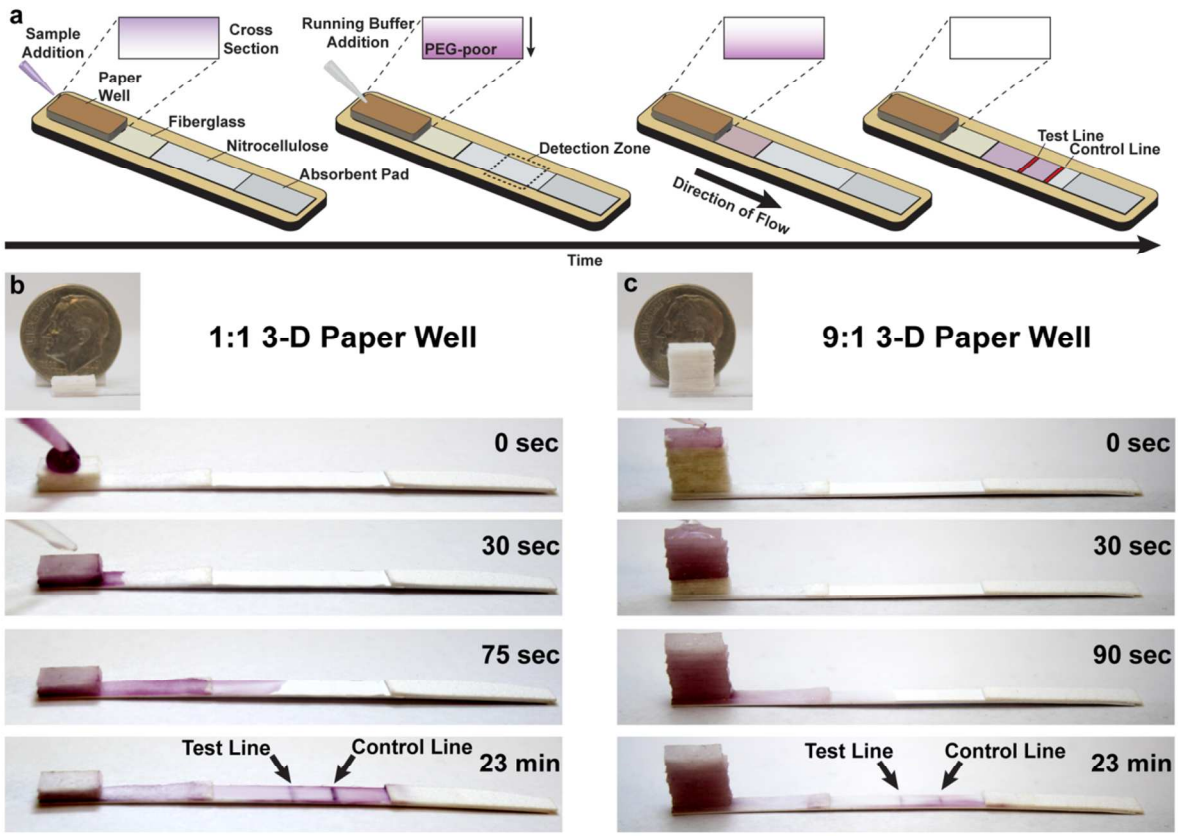

Figure 4: *The 3-D paper well was combined with ATPS and LFA for Tf detection*. (a) The paper well

device was combined with the Tf competition assay on nitrocellulose paper. Samples containing no Tf were correctly diagnosed when using the (b) 1:1 or (c) 9:1 volume ratio ATPS solutions with visible test and control lines.

After verifying that the 3-D paper well can be combined with LFA to accurately assess the absence of Tf in negative control ATPS samples, the Tf concentrations were varied to find the detection limits when using the 1:1 and 9:1 volume ratio ATPS solutions. As predicted, these experiments demonstrated 2-fold and 10-fold improvements in the detection limit of Tf over conventional LFA, respectively (Fig. 5). For the 9:1 volume ratio ATPS experiments with the 3-D paper well, the sample was allowed to incubate within the device for an additional 10 min to allow ample time for the DGNPs to capture the target protein and phase separate macroscopically before addition of the running buffer. Note that this incubation period was not required for the 1:1 volume ratio ATPS because the DGNPs were more concentrated in the mixed ATPS, making it easier for the DGNPs to probe the entire solution. The results of these experiments showed that, while conventional LFA detected Tf at concentrations of 1 ng/uL (concentration at which no test line appears), our 3-D paper-based diagnostic device was capable of detecting Tf at 0.5 ng/uL (2-fold improvement in the detection limit) when the 1:1 volume ratio ATPS was used. Similarly, the 3-D paper-based diagnostic device was capable of detecting Tf at 0.1 ng/uL (10-fold improvement in the detection limit) when the 9:1 volume ratio ATPS was used. These results suggest that an ATPS solution with the desired volume ratio can be combined with an appropriately sized 3-D paper well to significantly and predictably improve the biomarker detection using LFA.

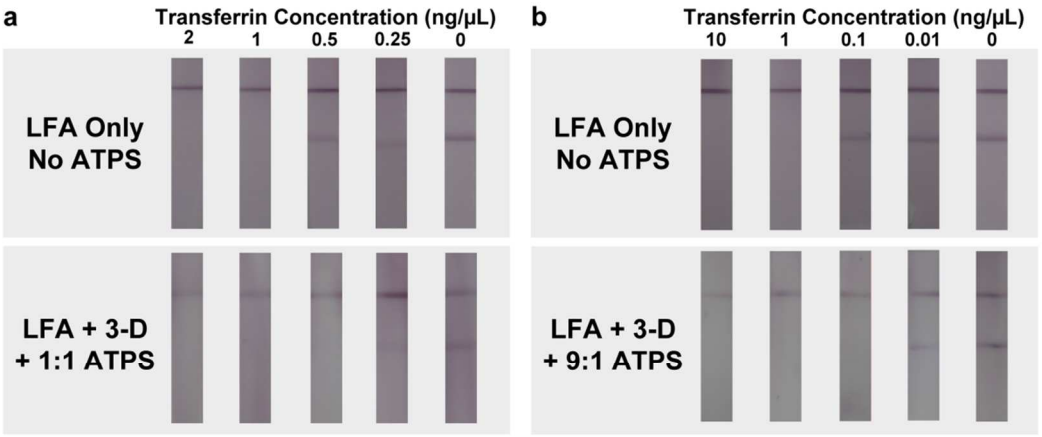

Figure 5: *The 1:1 volume ratio ATPS with the 3-D paper well allows for a 2-fold improvement in the detection limit of Tf while the 9:1 volume ratio ATPS allows for a 10-fold improvement.* (a) Conventional LFA detected Tf at 1 ng/μL but could not detect Tf at 0.5 ng/μL, resulting in a false negative. A 1:1 volume ratio ATPS with the 3-D paper well successfully detected Tf at 0.5 ng/μL. (b) Conventional LFA detected Tf at 1 ng/μL but could not detect Tf at 0.1 ng/μL, resulting in a false negative. A 9:1 volume ratio ATPS with the 3-D paper well successfully detected Tf at 0.1 ng/μL.

Conclusion

In the current study, we have demonstrated that our 3-D paper-based diagnostic device allows for the direct addition of an ATPS and results in a 10-fold improvement in the detection limit of a model protein Tf. A mixed ATPS applied directly to the paper membrane rapidly phase separates as it flows through the device, simultaneously allowing biomarker concentration and downstream detection with a reduced time-to-result. Although the precise mechanism for enhanced ATPS phase separation in paper still requires further investigation, we have shown that the paper speeds up the ATPS phase separation behavior and that 3-D paper architectures can further enhance this phenomenon in ways that a simple 2-D structure cannot accomplish. Expanding into the vertical dimension with the paper well enables processing of larger sample volumes and

allows gravitational forces to aid in the phase separation, while the multiple layers of fiberglass membrane provide a greater cross-sectional area through which the domains of the ATPS can interact. In the future, we are interested in studying this phase separation in paper phenomenon by determining the fundamental principles of the paper that drive this action.

Our 3-D paper diagnostic is the first to demonstrate ATPS phase separation in paper, allowing for concentration of the target analyte as the sample flows through the paper to the downstream detection zone. This implementation improves the sensitivity of conventional LFA devices while maintaining ease-of-use and time-to-result. With 10-fold improvements in detection limit, our device has the potential to rapidly identify pathogens at lower concentrations that were previously undetectable with conventional LFA. This robust and portable device requires no electricity or sophisticated laboratory equipment and is ideal for POC applications in resource-poor settings. The 3-D paper architecture can also easily be applied to existing commercial LFA products, transforming them to next-generation rapid diagnostics without inheriting the poor sensitivity characteristic of conventional LFA. Once fully developed, this platform technology has the potential to revolutionize the state of health care in resource-poor settings by providing rapid, accurate, and inexpensive diagnostics, leading to improved patient management, treatment, and outbreak prevention.

Conflict of Interest

R.Y.T. Chiu and D.T. Kamei are founders of a company that intends on commercializing this core technology.

Acknowledgments

This work was supported by UCLA funds.

References

1. P. Yager, G. J. Domingo and J. Gerdes, *Annu Rev Biomed Eng*, 2008, 10, 107-144.
2. World Health Organization., World Health Organization, Geneva, Switzerland.
3. C. A. Petti, C. R. Polage, T. C. Quinn, A. R. Ronald and M. A. Sande, *Clin Infect Dis*, 2006, 42, 377-382.
4. P. Yager, T. Edwards, E. Fu, K. Helton, K. Nelson, M. R. Tam and B. H. Weigl, *Nature*, 2006, 442, 412-418.
5. E. Fu, T. Liang, J. Houghtaling, S. Ramachandran, S. A. Ramsey, B. Lutz and P. Yager, *Anal Chem*, 2011, 83, 7941-7946.
6. E. Fu, T. Liang, P. Spicar-Mihalic, J. Houghtaling, S. Ramachandran and P. Yager, *Anal Chem*, 2012, 84, 4574-4579.
7. C. M. Cheng, A. W. Martinez, J. Gong, C. R. Mace, S. T. Phillips, E. Carrilho, K. A. Mirica and G. M. Whitesides, *Angew Chem Int Ed Engl*, 2010, 49, 4771-4774.
8. J. L. Osborn, B. Lutz, E. Fu, P. Kauffman, D. Y. Stevens and P. Yager, *Lab on a Chip*, 2010, 10, 2659-2665.
9. H. Noh and S. T. Phillips, *Anal Chem*, 2010, 82, 4181-4187.
10. B. R. Lutz, P. Trinh, C. Ball, E. Fu and P. Yager, *Lab on a Chip*, 2011, 11, 4274-4278.
11. H. Noh and S. T. Phillips, *Anal Chem*, 2010, 82, 8071-8078.
12. B. Lutz, T. Liang, E. Fu, S. Ramachandran, P. Kauffman and P. Yager, *Lab on a Chip*, 2013, 13, 2840-2847.
13. X. Li, P. Zwanenburg and X. Liu, *Lab on a Chip*, 2013, 13, 2609-2614.
14. F. Mashayekhi, R. Y. Chiu, A. M. Le, F. C. Chao, B. M. Wu and D. T. Kamei, *Anal Bioanal Chem*, 2010, 398, 2955-2961.
15. F. Mashayekhi, A. M. Le, P. M. Nafisi, B. M. Wu and D. T. Kamei, *Anal Bioanal Chem*, 2012, 404, 2057-2066.
16. H. Jang, S. R. Ryoo, K. Kostarelos, S. W. Han and D. H. Min, *Biomaterials*, 2013, 34, 3503-3510.
17. P. N. Njoki, I. I. S. Lim, D. Mott, H. Y. Park, B. Khan, S. Mishra, R. Sujakumar, J. Luo and C. J. Zhong, *J Phys Chem C*, 2007, 111, 14664-14669.
18. M. C. Daniel and D. Astruc, *Chem Rev*, 2004, 104, 293-346.
19. R. Y. Chiu, P. T. Nguyen, J. Wang, E. Jue, B. M. Wu and D. T. Kamei, *Annals of biomedical engineering*, 2014, DOI: 10.1007/s10439-10014-11043-10433.

Footnotes

*Electronic supplementary information (ESI) available: Fabrication and performance of the triggered well device and videos of the 1:1 and 9:1 volume ratio ATPS solutions with dyes traveling through the triggered well device, a paper membrane, and a 3-D paper well.

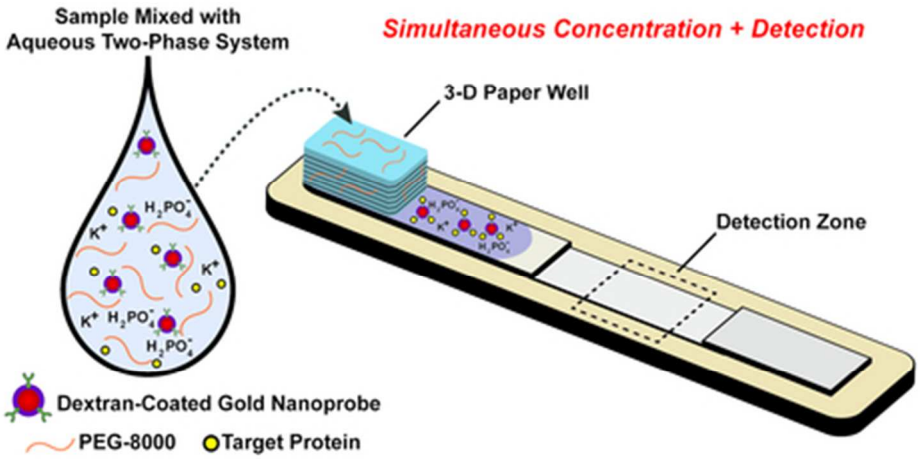

39x19mm (300 x 300 DPI)